

RESEARCH ARTICLE

Analysis of Self-Similar Solutions of Euler System: SIB, Desingularization and Impasse Points

WIESLAW MARSZALEK 

Department of Computer Science, Opole University of Technology, 45-758 Opole, Poland

e-mail: w.marszalek@po.edu.pl


ABSTRACT This paper shows that the singularity induced bifurcation (SIB) phenomenon and desingularization tool from nonlinear differential-algebraic equations (DAEs) are intrinsic parts of the compressible model of Euler flow in the self-similar framework. The nonlinear DAEs in such a setting include the crossings of sonic (singularity) points by a smooth trajectory. The linearization of DAEs around the sonic points is characterized by the divergence of eigenvalues through infinity and a presence of *folded* nodes. Also, the singularity manifold includes mostly the impasse points, where trajectory collapses at or originates from. The desingularization tool from DAEs results in a singularity-free model, that is a system of ordinary differential equations (ODEs), having *regular* nodes as its equilibria. Partial reversal of the direction of the independent self-similar variable results in a transformation of the *regular* nodes into *folded* ones for the original Euler DAE system. The Euler DAE system is a system of DAEs obtained after the similarity variable $x = t/r^\lambda$ is applied in the Euler systems of three partial differential equations for conservation of mass, balance of momentum, and balance of energy. The smooth trajectory connecting two equilibria of the Euler DAE system passes through two sonic points, traversing through the super- and subsonic areas for the independent self-similar variable $-\infty < x < \infty$. The point $x = 0$ is also of an interesting nature, with an infinite number of possible smooth trajectories passing through it. The analysis is based on a combination of both analytic and numeric approaches. Overall, the paper links the topics from the areas of fluid flows (in the Eulerian framework), self-similar solutions and DAEs.

INDEX TERMS Compressible Euler flow, desingularization, nonlinear singular (implicit) models, self-similar solutions, singularity induced bifurcations, transonic flows.

I. INTRODUCTION

A. A BRIEF HISTORICAL PERSPECTIVE

Similar and self-similar solutions are of great importance in many physical and engineering systems since the middle of the last century, see for example [1], [2], [3], [4], [5]. At the same time it has been recognized that the behavior of various flows around Mach-1 (sonic) speeds in astrophysics, aeroelasticity and magnetohydrodynamics is not well-understood. Both facts lead to significant research efforts being undertaken in the area of transonic flows [6], [7], [8], [9], [10], [11], [12], [13]. Such efforts are still being continued in the current years. Shock and shockless solutions in transonic flows and their properties

The associate editor coordinating the review of this manuscript and approving it for publication was Ludovico Minati .

result in complex mathematical methods and techniques being employed [14], [15], [16], [17], [18], [19], [20], [21], [22], as one often needs to consider the *sonic manifolds* of the underlying models as their *singularities* [23], [24], [25], [26], [27]. The complexity of the problems being analyzed is challenging on one side (for example when numerical aspects of the transonic solutions in semi-similar problems are considered), but it also offers new opportunities to bring various methods and techniques from different research areas into the self-similar transonic flow problems. This paper is one of such attempts, as the phenomena of the singularity induced bifurcations and desingularizations from the dynamical systems described by implicit ODEs, sometimes called the DAEs (or Differential-Algebraic Equations), are being used here in the analysis of transonic self-similar solutions of the compressible Euler system. Such

a treatment of the Euler system is new, interesting, and has not been reported in the literature.

B. THE PRESENT APPROACH: FOSTERING OF CROSS-FERTILIZATION OF IDEAS AND TECHNIQUES

This paper shows that the DAEs that result from the self-similar approach to the compressible Euler system have many typical properties and features of implicit ODEs in nonlinear dynamical systems. In particular, the singularity manifold of the Euler DAEs consists of both the *algebraic* and *geometric* points, with the former behaving as impasse points, while the later allowing for smooth crossings of the singularity manifold. Thus, in practice, for the *geometric* points the equilibrium property and singularity are both lost, allowing for smooth flow transition. The *desingularization* of the self-similar Euler DAEs is also possible. In such a case, the *geometric* points of the Euler DAEs are transformed into *regular* equilibria of the node type of the *desingularized* nonlinear DAEs. The term *desingularized* DAEs is used when a DAE system with singularities becomes an ODE system via a transformation of variables. The trajectories of the *desingularized* DAEs have partially reversed directions, resulting in the *regular* repelling nodes with positive eigenvalues.

The above issues are presented in this paper through a combination of analytical and numerical results and our approach is believed to be an alternative to that presented elsewhere, for example in [14], where neither the DAE tools (i.e. the singularity-induced bifurcation) nor the *desingularization* of DAEs have been used.

It is believed that the DAE approach presented in this paper can also be applied to the self-similar implicit equations in other areas, such as, for example in the computation of transonic self-similar flows in the spherically symmetric gravitational field by a point mass considered in [15] and [16], subsonic-supersonic transitions of aeroelastic airfoils [17], [18], and interactions between flutter and buffet in transonic flows [19], [20].

II. THE EULER SYSTEM AND ITS SELF-SIMILAR MODEL

In this paper we chose to deal with the issues described in the second part of the Introduction in the context of the Euler system in fluid flows to make the presentation self-contained and complete. However, it is believed that the issues discussed here can also be considered in the framework of the Lagrangian system. The compressible flow in the Euler framework is described by the equations for conservation of mass, balance of momentum, and balance of energy, plus a constitutive equation for the specific energy density of the fluid. Our system is non-isentropic as being more realistic and allowing for changes of entropy.

The non-isentropic compressible Euler system in two ($n = 2$) or three ($n = 3$) dimensions has the form [14]

$$\rho_t + u\rho_r + \rho(u_r + \frac{n-1}{r}u) = 0$$

$$\begin{aligned} u_t + uu_r + \frac{1}{\gamma\rho}(\rho c^2)_r &= 0 \\ c_t + uc_r + \frac{\gamma-1}{2}c(u_r + \frac{n-1}{r}u) &= 0 \end{aligned} \tag{1}$$

where the density $\rho := \rho(t, r)$, velocity field is radial, that is, $u = u_r^x$ for $r = |x|$, $u := u(t, r)$, and the local speed $c := c(t, r)$ is such that $c = \sqrt{\frac{\gamma p}{\rho}} = \sqrt{\gamma(\gamma-1)e}$, with e being the internal energy (component of the total energy $E = e + \frac{1}{2}|u|^2$), and $\gamma > 1$ is the adiabatic constant.

When we look for semi-similar solution with parameters λ and κ in the independent variable $x = t/r^\lambda$ with the dependent variables $\rho(t, r) = r^\kappa R(x)$, $u(t, r) = -\frac{r^{1-\lambda}}{\lambda x} V(x)$ and $c(t, r) = -\frac{r^{1-\lambda}}{\lambda x} C(x)$, then the following ODE system is obtained [14]

$$\begin{aligned} \lambda x D(V, C) \frac{dV}{dx} &= -G(V, C) \\ \lambda x D(V, C) \frac{dC}{dx} &= -F(V, C) \end{aligned} \tag{2}$$

with

$$\begin{aligned} D(V, C) &= (1+V)^2 - C^2 \\ G(V, C) &= nC^2(V - V_*) - V(1+V)(\lambda + V) \\ F(V, C) &= C\{C^2(1 + \frac{\alpha}{1+V}) - k_1(1+V)^2 \\ &\quad + k_2(1+V) - k_3\} \end{aligned} \tag{3}$$

where $V_* = \frac{\kappa-2(\lambda-1)}{n\gamma}$, $\alpha = \frac{1}{2\gamma}[\kappa(\gamma-1) + 2(\lambda-1)]$, and

$$\begin{aligned} k_1 &= 1 + \frac{(n-1)(\gamma-1)}{2} \\ k_2 &= \frac{(n-1)(\gamma-1) + (\gamma-3)(\lambda-1)}{2} \\ k_3 &= \frac{(\gamma-1)(\lambda-1)}{2}. \end{aligned} \tag{4}$$

Analyzing system (2)-(4) and its properties around various points in the plane (C, V) is the topic of this paper. The *singularity* of the above system occurs for those points in the plane where $D(V, C) = 0$ or $x = 0$. The points $D(V, C) = 0$ and $x \neq 0$ behave mostly as the *impasse* points [23], [24]. However, when additional conditions are added, namely, $G(V, C) = 0$ and $F(V, C) = 0$, then we obtain the *singular equilibria*. Those points in the (C, V) plane where $G(V, C) = 0$ and $F(V, C) = 0$, but $D(V, C) \neq 0$, are *regular equilibria*. The (t, r) values where the similarity independent variable x is 0 is also of special interest (see section III-B).

The most interesting points (C, V) are the *singular equilibria* located on two straight lines $C = \pm(V + 1)$. These points are called the *sonic* points and can be used to compute a smooth solution connecting two equilibria at $(V_*, \pm\infty)$, and passing through the origin $(C, V) = (0, 0)$ exactly when $x = 0$. Notice that for $x = 0$ we have the coefficients of the derivatives on the left-hand side in (2) equal 0. Additionally, since the smooth solution of (2) is constructed in such a way that for $x = 0$ we have $V(0) = C(0) = 0$, therefore both

the G and F in (3) are also zero when $x = 0$. The above facts result in very interesting and intriguing properties of (2)-(4) to be analyzed in the next sections.

Summary of the Main Findings (in the Three Sections to Follow):

- The singularity $D(V, C) = 0$ in (2) yields two lines $C = \pm(V + 1)$, which, together with the line $C = 0$, divide the whole (C, V) space into four areas that are important in the desingularization of (2)-(4). When a desingularized system of (2)-(4) is analyzed, then the direction of the vector field and solution orbits in two of those four areas are reversed.
- The reversing of the direction of the semi-similar variable x and vector field is due to a specially applied diffeomorphism used in the process of obtaining a smooth solution connecting $(V_*, +\infty)$ with $(V_*, -\infty)$. Two of the four areas where the reversing is needed are those where $x D(V, C) < 0$ (see the left-hand sides of (2)). In one of those two areas we have $x < 0$ and $C^2 - (1 + V)^2 > 0$, while in the second area we have $x > 0$ and $C^2 - (1 + V)^2 < 0$. The two such areas are marked by the yellow color in Figs.1 and 2(a). In two other areas (the white color) no reversal of the x -direction and vector field should be done, as both those areas are such that $x D(V, C) > 0$.
- The singularity-induced bifurcations present in the Euler system (2) results in the divergence of eigenvalues of the linearized Euler DAEs through $\pm\infty$. The linear model is stable on one side of the singularity and unstable on the other side. This yields folded nodes of the linearized system (2)-(4).

The above issues are discussed in the next three sections in this paper. The desingularization and SIB phenomena have not been discussed in the literature analyzing the self-similar Euler system (1) thus far, but are quite helpful in determining the overall solution of (2)-(4), particularly in finding the smooth trajectory passing through the transonic points. The smooth trajectory is constructed thanks to a special diffeomorphism used to transform the self-similar variable x . Such transformation allows us to obtain a solution that passes through the transonic points A and B (see Figs.1(b) and 2(b)) and through the origin when $x = 0$. The solutions in the upper half of the plane (with $C > 0$) are for $x < 0$, while those in the lower half (with $C < 0$) are for $x > 0$.

III. LINEAR MATRIX PENCIL OF (2) AROUND SINGULAR POINTS $D(V, C) = 0$ AND $x = 0$

A. DIVERGENCE OF EIGENVALUES THROUGH INFINITY AT GEOMETRIC SINGULAR POINTS WITH $D(V, C) = 0$

When the Euler DAE model (2) is linearized, one obtains

$$\lambda x D(V, C) \begin{pmatrix} \frac{dV}{dx} \\ \frac{dC}{dx} \end{pmatrix} = \begin{pmatrix} -\frac{\partial G}{\partial V} & -\frac{\partial G}{\partial C} \\ -\frac{\partial F}{\partial V} & -\frac{\partial F}{\partial C} \end{pmatrix} \begin{pmatrix} V \\ C \end{pmatrix} \quad (5)$$

with the linear matrix pencil

$$\{A, L\} := \left\{ \lambda x D(V, C) \begin{pmatrix} 1 & 0 \\ 0 & 1 \end{pmatrix}, \begin{pmatrix} -\frac{\partial G}{\partial V} & -\frac{\partial G}{\partial C} \\ -\frac{\partial F}{\partial V} & -\frac{\partial F}{\partial C} \end{pmatrix} \right\} \quad (6)$$

having the determinant

$$\begin{aligned} \det(sA - L) &= s^2 \lambda^2 x^2 D^2(V, C) \\ &+ s \lambda x D(V, C) \left(\frac{\partial F}{\partial C} + \frac{\partial G}{\partial V} \right) + \frac{\partial F}{\partial C} \frac{\partial G}{\partial V} - \frac{\partial F}{\partial V} \frac{\partial G}{\partial C} e \end{aligned}$$

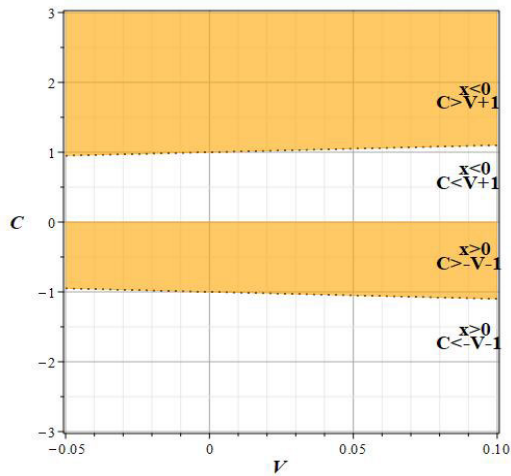
and the eigenvalues $s_{1,2}$ obtained from $\det(sA - L) = 0$ diverging through infinity, that is, $s_{1,2} \rightarrow \pm\infty$ when $(1 + V)^2 - C^2 \rightarrow 0$ (solution trajectory approaches transonic points A or B in Figs.1(b) and 2(a)). This fact follows from the property of the above quadratic polynomial, with the coefficients of s^2 and s being zero at the sonic points A and B (because $D(V, C) = 0$ at those points). Since $\frac{\partial F}{\partial V} \frac{\partial G}{\partial C} - \frac{\partial F}{\partial C} \frac{\partial G}{\partial V} \neq 0$ (see section IV), then calculating the eigenvalues s_1 and s_2 , we obtain

$$s_{1,2} = \frac{-\left(\frac{\partial F}{\partial C} + \frac{\partial G}{\partial V}\right) \pm \sqrt{\left(\frac{\partial F}{\partial C} + \frac{\partial G}{\partial V}\right)^2 - 4\left(\frac{\partial F}{\partial C} \frac{\partial G}{\partial V} - \frac{\partial F}{\partial V} \frac{\partial G}{\partial C}\right)}}{2x D(V, C)} \quad (7)$$

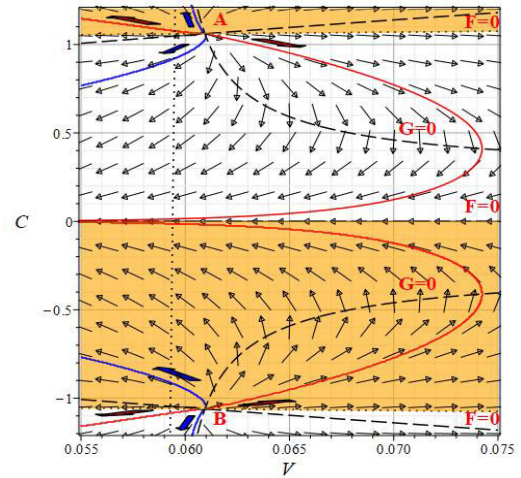
from which it follows that the numerators of both s_1 and s_2 are different than 0 at the transonic points A and B . Thus, each of the eigenvalues s_1 and s_2 diverges through $\pm\infty$ in a special way. Since the denominator is zero at the singularity $C = \pm(V + 1)$, therefore $\lim_{x \rightarrow x^*} |s_{1,2}| \rightarrow \infty$ with x^* denoting the self-similarity independent variable values at either point A or B . Because the denominator in the expressions for $s_{1,2}$ changes sign at both A and B , therefore we say that the eigenvalues diverge through $\pm\infty$ at the transonic points A and B . Thus, the linear model has stable-unstable (or unstable-stable) character near the points A and B . This is exactly the same phenomenon discussed in the context of many nonlinear DAEs, for example, those in electric power systems, traveling waves in magnetohydrodynamics, economy and others, see for example [25], [26], [27].

B. SINGULAR POINT $x = 0$

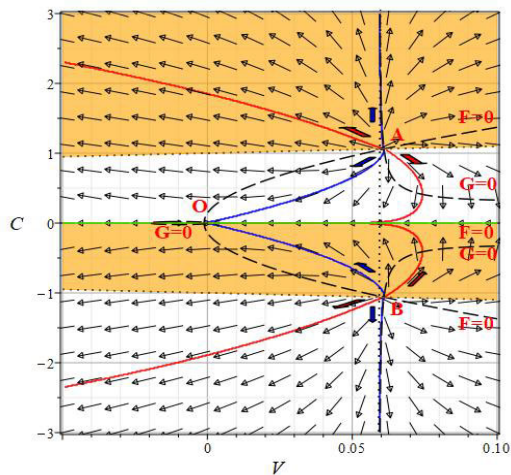
When a trajectory approaches $x = 0$ (for $t = 0, r \neq 0$), then (2) yields the linearization $\frac{dC}{dV} = \frac{C}{V}$, with a proper node at $(C, V) = (0, 0)$. Any trajectory approaching $(0, 0)$ reaches that point at $x = 0$ with finite limits $\lim_{x \rightarrow 0} \frac{V(x)}{x}$ and $\lim_{x \rightarrow 0} \frac{C(x)}{x}$. Two such trajectories are shown for illustration in Fig.2(b). When the flow in the yellow part of the (C, V) plane is reversed for (2)-(4), then each such a solution will pass from the upper part (for $x < 0$, the white half-plane) to the lower part (for $x > 0$), reaching the origin O at $x = 0$. There is an infinite number of possible smooth trajectories



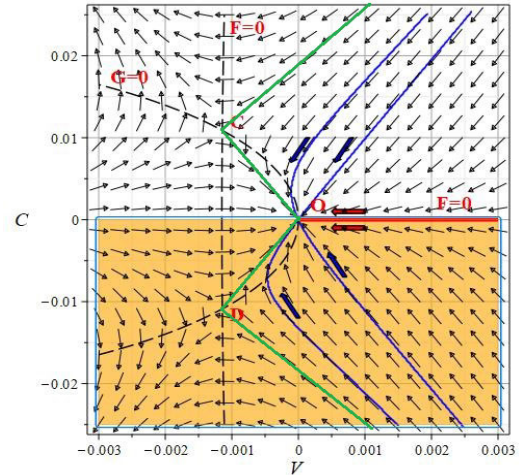
(a) Four areas of the (C, V) space.



(a) As in Fig.1(b) for $|C| \leq 1.2$ and $0.055 \leq V \leq 0.075$.



(b) Dynamic features of the Euler *desingularized* DAE system.



(b) Dynamic features of the Euler *desingularized* DAE system around the origin.

FIGURE 1. (a) The (C, V) space is divided by the singularity $x[(1 + V)^2 - C^2] = 0$ (two dotted lines and $C = 0$) into four areas. (b) The flow of the *desingularized* Euler system must be reversed in the yellow highlighted areas in order to obtain actual flow of (2), (3). We have $x[(1 + V)^2 - C^2] < 0$ in those two areas with the reversed flow direction. It is assumed that the independent self-similar variable $-\infty < x < 0$ in the upper half-plane (with $C > 0$) and $0 < x < \infty$ in the lower half-plane (with $C < 0$), as well as the solution trajectory $(C(x), V(x))$ is such that $(C(0), V(0)) = (0, 0)$. Thus, the solution of (2) passes through the origin when $x = 0$.

passing through $(0, 0)$ at $x = 0$ and bounded by the *separatrices* of the saddle points C and D . Those separatrices (green solid lines in Fig.2(b)) are the eigendirections of the two saddle points. Notice that the two trajectories through the origin O are not symmetrical with respect to the line $C = 0$. However, in a special case, such a symmetric trajectory may occur with a vertical passing of the trajectory through the origin O and vanishing $\lim_{x \rightarrow 0} \frac{V(x)}{x}$.

IV. DESINGULARIZED EULER DAE MODEL AND ITS EIGENVALUES: DIRECTION OF FLOW

By using the *desingularized* Euler DAE model with $G(V, C)$ and $F(V, C)$, the linearization of that model around the

FIGURE 2. Phase portrait and important dynamical features of the *desingularized* semi-similar Euler system. In Fig.2(b) two (of many possible) trajectories passing through the origin are shown (blue solid curves). All such trajectories are bounded by the separatrices - the eigendirections of two saddle points at C and D (green solid segments). The two saddles (due to $G = F = 0$ and $D \neq 0$) are neither located on the singularity $(1 + V)^2 - C^2 = 0$ nor do they occur at $x = 0$.

the transonic points can be analyzed through the linearized matrix (see [16])

$$\mathcal{T} = \begin{pmatrix} \lambda \frac{\partial(xD)}{\partial x} & \lambda \frac{\partial(xD)}{\partial V} & \lambda \frac{\partial(xD)}{\partial C} \\ -\frac{\partial G}{\partial x} & -\frac{\partial G}{\partial V} & -\frac{\partial G}{\partial C} \\ -\frac{\partial F}{\partial x} & -\frac{\partial F}{\partial V} & -\frac{\partial F}{\partial C} \end{pmatrix} = \begin{pmatrix} \lambda[(1 + V)^2 - C^2] & 2\lambda x(1 + V) & -2\lambda x C \\ 0 & -\frac{\partial G}{\partial V} & -\frac{\partial G}{\partial C} \\ 0 & -\frac{\partial F}{\partial V} & -\frac{\partial F}{\partial C} \end{pmatrix}$$

whose singularity is due to the fact that $\frac{\partial(xD)}{\partial x} = 0$ at the *sonic* points A and B , and the characteristic equation $\det(sI - T) = 0$ at those points is

$$s \left[\left(s + \frac{\partial G}{\partial V} \right) \left(s + \frac{\partial F}{\partial C} \right) - \frac{\partial G}{\partial C} \frac{\partial F}{\partial V} \right] = 0 \quad (8)$$

The matrix T and the two of its non-zero eigenvalues describe the dynamics of the *desingularized* Euler DAEs in the following way: to determine the local behavior around the transonic points with $(1+V)^2 - C^2 = 0$ one needs to compute the two non-zero eigenvalues of T , change the signs of those eigenvalues of T to opposite when $x[(C^2 - (1+V)^2)] < 0$ (the yellow-highlighted areas in Figs. 1 and 2(a)) and keep the signs unchanged when $x[(C^2 - (1+V)^2)] > 0$ (see section V for an explanation).

For the two transonic points A and B shown in Figs. 1(b) and 2(a) we obtain identical characteristic equations (with 6 decimal digits for the eigenvalues): $s(s - 2.541993)(s - 2.930548) = 0$, confirming the fact that T describes the *desingularized* system with two real positive eigenvalues at both points A and B (resulting in two *regular node* points in Figs. 1(b) and 2(a)). This further yields, after changing the direction of trajectories for $x[(C^2 - (1+V)^2)] < 0$ (yellow-highlighted areas in Fig. 2), the *folded node* character of both transonic points for (2), (3). Such a useful *desingularization* process of getting T for the *desingularized* Euler DAEs and using it to obtain *folded nodes* from the *regular* ones, is described in more details, among others, in [26]. Further details of the solutions in Fig. 2 are provided in the caption of that figure.

V. THE SINGULARITY (OR SONIC) CROSSING TRAJECTORY

The singularity crossing for (2)-(4) falls into the framework considered in [26], since the present model has the *quasilinear* DAE form

$$A(x, u(x))u' = b(x, u(x)) \quad (9)$$

where $(\cdot)' \equiv d/dx$ and $u(x) \equiv (V, C)^T$. The *transonic* points are those *geometric* singularities $u^* := u(x_c)$ of that DAE system with $b(x_c, u^*) \in \mathfrak{S}A(x_c, u^*)$, for which [26, Theorem 1] is applicable, leading to the conclusion of the existence of smooth C^1 *transonic* solutions. Here, $\mathfrak{S}A(x_c, u^*)$ denotes the image of $A(x_c, u^*)$. The local diffeomorphism used in [26, page 306] to obtain smooth *transonic* solution through u^* is the reason for reversing of the x -direction when analyzing the solutions of (2) and its *desingularized* ODE model. For example, the diffeomorphism for (2) with singularity $xD(V, C) = 0$ is the integral $\xi(x) = \int_0^x \lambda x D(\tau, y(\tau)) d\tau$, where $y(x)$ is the solution of $y' = -(G, F)^T$, $y(0) = u^*$. When $xD(V, C) > 0$ around u^* (the white areas in Fig. 1 and 2), then $\xi(x)$ is increasing and the integral curves of $-(G, F)$ are mapped into those of $-(G, F)/(\lambda x D)$ with the x -orientation (direction) being preserved. When $xD(V, C) < 0$ near x^* (the yellow areas in Figs. 1 and 2), then $\xi(x)$ is decreasing, and the x -orientation

(direction) is reversed along trajectories in those regions. The two integral curves emanating from u^* are used to obtain a C^1 trajectory satisfying $u(x_c) = u^*$. Such a reversal of the x -directions occurring in the appropriate regions results in the reversals of the orbits of the *regular nodes* at the points A and B to yield the *folded nodes* for (2). See [26, page 307] for more details and [28] for a similar discussion on this topic.

Finally, it should be emphasized that the smooth solutions through the points A , B and O in Figs. 1 and 2 (the red and blue ones) were obtained by glueing the partial solutions obtained along the eigen-directions determined at the three points of interest, with the initial conditions selected very close to those points (distance of order 10^{-4} from the points) and the relative and absolute errors of the *ode45* solver equal to 10^{-8} .

VI. CONCLUSION

When the Euler self-similar flow crosses the *singularity* manifold $D(V, C) = 0$ at the singular *geometric* points, the SIB phenomenon occurs. Such crossings happen twice (at points A and B) by a single trajectory in the considered self-similar Euler framework, as illustrated in this paper. On the other hand, when the SIB is not present at a singular point $D(V, C) = 0$ (*algebraic* singularity), then that point is an *impasse* point, where the self-similar solution flow ceases to exist or where the flow originates from. When the singularity is removed (through the *desingularization* process), then the *desingularized* Euler ODE has *regular* equilibrium points (unstable nodes) and no *impasse* points are present. Such tools and methods are applied in other areas of science and engineering. For example, the electric power system modeling furnishes examples of the system undergoing dramatic changes and lost stability through the existence of *geometric* points on the singularity manifold. Researchers attempt to explain the collapsing electric power systems [29], by using the *singularity* crossing phenomena [25], [28]. Also, [26] and [30] include similar results in the two-phase flows and inviscid transonic flows, respectively.

Finally, it is believed that the approach presented in this paper can also be applied in the Lagrangian formulation of the self-similar fluid flows, and a comparison analysis of the properties of the Lagrangian versus Euler DAEs would be interesting to be seen.

REFERENCES

- [1] L. I. Sedov, *Similarity and Dimensional Methods in Mechanics*, 10th ed. Boca Raton, FL, USA: CRC Press, 1993.
- [2] A. D. Bruno, "Self-similar solutions," in *North-Holland Mathematical Library*, vol. 57. Amsterdam, Holland: Elsevier, 2000, pp. 315–340.
- [3] A. Biasi, "Self-similar solutions to the compressible Euler equations and their instabilities," *Commun. Nonl. Sci. Numer. Simul.*, vol. 103, Dec. 2021, Art. no. 106014.
- [4] W. G. Vincenti, "Engineering theory in the making: Aerodynamic calculation," breaks the sound barrier," *Technol. Culture*, vol. 38, no. 4, pp. 819–851, Oct. 1997, doi: 10.2307/3106951.
- [5] J. Eggers and M. A. Fontelos, "The role of self-similarity in singularities of PDE's," 2008, *arXiv:0812.1339*.
- [6] A. I. Ruban, *Transonic Flows*. Oxford, U.K.: Oxford Univ. Press, 2015, doi: 10.1093/acprof:oso/9780199681747.003.0005.

- [7] (2015). *Mach 1 Airspace*. [Online]. Available: <https://www.youtube.com/watch?v=e8kUf8HSu3k>
- [8] (2010). *Supersonic Flight, Sonic Booms*. [Online]. Available: <https://www.youtube.com/watch?v=gWGLAAYdbbc>
- [9] H. J. Ramm, *Fluid Dynamics for the Study of Transonic Flow*. New York, NY, USA: Oxford Univ. Press, 1990.
- [10] S. Chakrabarti, *Theory of Transonic Astrophysical Flows*. Singapore: World Scientific, 1990.
- [11] C. Gao and W. Zhang, "Transonic aeroelasticity: A new perspective from the fluid mode," *Prog. Aerosp. Sci.*, vol. 113, Feb. 2020, Art. no. 100596.
- [12] B. I. Epureanu, E. H. Dowell, and K. C. Hall, "Reduced-order models of unsteady transonic viscous flows in turbomachinery," *J. Fluids Struct.*, vol. 14, no. 8, pp. 1215–1234, Nov. 2000.
- [13] K. C. Hall, W. S. Clark, and C. B. Lorence, "A linearized Euler analysis of unsteady transonic flows in turbomachinery," *J. Turbomachinery*, vol. 116, no. 3, pp. 477–488, Jul. 1994.
- [14] H. K. Jenssen and A. A. Johnson, "New self-similar Euler flows: Gradient catastrophe without shock formation," 2022, *arXiv:2205.15876*.
- [15] A. F. Cheng, "Time-dependent fluid flow in a central gravitational field," *Astrophys. J.*, vol. 213, pp. 537–547, Apr. 1977.
- [16] J. Fukue, "Self-similar transonic flow in the spherically symmetric gravitational field," *Publ. Astron. Soc. Jpn.*, vol. 36, pp. 87–103, Jan. 1984.
- [17] E. W. Beans, "Shockless transition from supersonic to subsonic flow," *J. Propuls. Power*, vol. 11, no. 2, pp. 387–389, Mar. 1995.
- [18] S. He, Z. Yang, and Y. Gu, "Nonlinear dynamics of an aeroelastic airfoil with free-play in transonic flow," *Nonlinear Dyn.*, vol. 87, no. 4, pp. 2099–2125, Mar. 2017.
- [19] W. Zhang, C. Gao, Y. Liu, Z. Ye, and Y. Jiang, "The interaction between flutter and buffet in transonic flow," *Nonlinear Dyn.*, vol. 82, no. 4, pp. 1851–1865, Dec. 2015.
- [20] G. Schewe and H. Mai, "Experiments on transonic limit-cycle-flutter of a flexible swept wing," *J. Fluids Struct.*, vol. 84, pp. 153–170, Jan. 2019.
- [21] R. B. Lazarus, "Self-similar solutions for converging shocks and collapsing cavities," *SIAM J. Numer. Anal.*, vol. 18, no. 2, pp. 316–371, Apr. 1981.
- [22] X. Yao, R. Huang, and H. Hu, "Data-driven modeling of transonic unsteady flows and efficient analysis of fluid–structure stability," *J. Fluids Struct.*, vol. 111, May 2022, Art. no. 103549.
- [23] I. O. Chua and A.-C. Deng, "Impasse points—Part I: Numerical aspects," *Int. J. Circuit Theory Appl.*, vol. 17, no. 2, pp. 213–235, Apr. 1989.
- [24] R. Winkler, "On simple impasse points and their numerical computation," Institut Für Mathematik, Humboldt-Universität Berlin, Berlin, Germany, Tech. Rep. 94–15, 1994.
- [25] H. Kwatny, A. Pasrija, and L. Bahar, "Static bifurcations in electric power networks: Loss of steady-state stability and voltage collapse," *IEEE Trans. Circuits Syst.*, vol. CS-33, no. 10, pp. 981–991, Oct. 1986.
- [26] W. Marszalek, T. Amdeberhan, and R. Riaza, "Singularity crossing phenomena in DAEs: A two-phase fluid flow application case study," *Comput. Math. With Appl.*, vol. 49, nos. 2–3, pp. 303–319, Jan. 2005.
- [27] W. Marszalek and Z. W. Trzaska, "Singularity-induced bifurcations in electrical power systems," *IEEE Trans. Power Syst.*, vol. 20, no. 1, pp. 312–320, Feb. 2005.
- [28] W. Marszalek, "A DAE approach to similarity solutions of unsteady fluid flows: An application case study," in *Proc. Amer. Control Conf.*, Jun. 2014, pp. 5145–5149.
- [29] B. Schäfer, D. Witthaut, M. Timme, and V. Latora, "Dynamically induced cascading failures in power grids," *Nature Commun.*, vol. 9, no. 1, p. 1975, May 2018.
- [30] W. Marszalek, "Fold points and singularity induced bifurcation in inviscid transonic flow," *Phys. Lett. A*, vol. 376, nos. 28–29, pp. 2032–2037, Jun. 2012.



WIESŁAW MARSZAŁEK received the Ph.D. and D.Sc. degrees in electrical engineering from the Warsaw University of Technology, Poland, and the Ph.D. degree in applied mathematics from North Carolina State University, Raleigh, NC, USA. In the past, he held various research and teaching positions with state and private universities in North Carolina, Ohio, New Jersey, and Connecticut (all in USA). He was a Humboldt Research Fellow in Bochum, Germany, from 1990 to 1992; Hamburg, Germany, in 1996; and Halle, Germany, in 2011; and a Fulbright Research Fellow in Warsaw, Poland, from 2005 to 2006; and Opole, Poland, in 2018. He currently teaches computer science and advises doctoral students with the Opole University of Technology, Poland. He is a reviewer for numerous international journals and conferences in engineering and applied mathematics. He has published more than 120 journals and conference papers in the areas of differential-algebraic equations, nonlinear circuits and electric arcs, memristors, singularity induced bifurcations, and chaos (see: <http://wmarszalek.weebly.com>).

• • •